

Face Recognition Application of Blur-Robust

Pitta Santhosh Kumar¹, Ankush Jain²

¹M.Tech student, Department of CSE, Anurag Group of Institutions, Hyderabad, India

²Assistant professor, Department of CSE, Anurag Group of Institutions, Hyderabad, India

Abstract: Understanding the effect of blur is an important problem in unconstrained visual analysis. We concentrate on this problem in the context of image-based recognition, by a fusion of image-formation models, as well as differential geometric tools. First, we talk about the space spanned by blurred versions of an image and then under certain assumptions, present a differential geometric analysis of that space. More exclusively, we create a subspace resulting from convolution of an image with a complete set of orthonormal basis functions of a pre-specified maximum size (that can represent an arbitrary blur kernel within that size), and explain that the equivalent subspaces created from a clean image and its blurred versions are equal under the ideal case of zero noise, and some assumptions on the properties of blur kernels. We then learn the practical utility of this subspace representation for the problem of direct recognition of blurred faces and by viewing the subspaces as points on the Grassmann manifold and present methods to perform recognition for cases where the blur is both homogenous and spatially varying. We empirically evaluate the effect of noise, as well as the presence of other facial variations between the gallery and probe images, and give comparisons with existing approaches on usual datasets.

Keywords: Blur Convolution, Subspace, Grassmann manifold, Face recognition.

1. Introduction

Understanding the effects of blur, which in general arise due to out-of-focus lens, atmospheric turbulence, and relative motion between the sensor and objects in the scene, is an important problem in image analysis applications such as face recognition. The image formation equation modeling the blurring process can be written as,

$$\tilde{y}(n_1, n_2) = (y * k)(n_1, n_2) + \eta(n_1, n_2) \quad (1)$$

where (n_1, n_2) denotes the pixel location at which a 2D convolution \times is performed between a $d_1 \times d_2$ clean image $y_{(d_1 \times d_2)}$ and an unknown blur point-spread function (PSF) $k_{(b_1 \times b_2)}$ to result in a blurred image $\tilde{y}_{(d_1 \times d_2)}$. The ubiquitous noise present in the system, which can be due to quantization, or other sensor induced errors, is represented by $\eta_{(d_1 \times d_2)}$. In recognition applications, existing methods to handle the effects of blur can be classified as: (i) inverse methods based on deblurring, and (ii) direct methods based on invariants.

The goal of deblurring is to estimate the clean image y from the observed blurred image \tilde{y} . Even with complete knowledge of the blur kernel k , an assumption which is hardly true in practice, inverting (1) to obtain y is an ill-posed problem due to the unknown nature of noise. Techniques for performing image restoration have been actively studied by the image processing community over the last four decades [4], and some of the prominent methodologies include: blind de-convolution [20] that does not assume any knowledge of the blur kernel, and thereby attempts to solve an under constrained problem of estimating both k and y from \tilde{y} , non-blind de-convolution which assumes models for blur [34], learning priors on clean image statistics [9], [19], and using coded-computational

photography techniques [2]. Regularization methods based on total variation [27] and Tikhonov regularization [31] constitute an integral part of this process. Such ideas have also been applied for recognizing faces across blur [17], [22], [23], [29].

In contrast to this, direct methods based on invariants search for those properties of the original image that are preserved across blur (under the assumption of zero noise). This is suited for applications where the goal is not to recover the clean image, but to extract features invariant to blur that can be used for subsequent tasks such as recognition or retrieval. Most efforts in this line of research are devoted to the specific class of centrally symmetric blur PSFs, which account for blur due to out-of-focus lens and atmospheric effects. The main observation behind these methods is as follows: Let \tilde{y}_F , y_F , and k_F denote the Fourier transform of \tilde{y} , y , and k respectively. Then under no noise, (1) can be written as $\tilde{y}_F(u, v) = y_F(u, v)k_F(u, v)$, where (u, v) denote the co-ordinates in frequency domain. The phase of these signals are related by $\angle \tilde{y}_F(u, v) = \angle y_F(u, v) + \angle k_F(u, v)$. Since centrally symmetric kernels have a phase of either 0 or π , the tangent of phase, $\tan(\angle \tilde{y}_F(u, v)) = \tan(\angle y_F(u, v))$, is invariant to blur. Using this property, moment-based invariants were derived both in spatial and Fourier domain, e.g. [11], [12]. Deriving invariants for linear motion blur has been addressed by [13]. There have been extensions of these works, which in addition to blur, accommodate invariance to rotation, similarity, and affine transformations [10], [30], and have been used for recognizing objects/ faces in distorted images [3], [24]. Robustness to noise is generally studied empirically.

Contributions: Our method belongs to the latter category. Unlike methods that impose restrictions on the parametric form of the blur kernel, we represent an arbitrary blur kernel as a linear combination of orthonormal basis functions that span the set of allowable blur kernels, and propose:

- A new blur invariant that handles more general class of blurs, by creating a subspace that results from convolution of an image with each individual basis function, which thereby contains (but not limited to) the set of all blurred versions of that image.
- We provide a differential geometric interpretation of the space spanned by these blur invariants, by studying them as points on a Grassmann manifold.
- We then utilize algorithms derived from this interpretation to perform face recognition across blur, where we demonstrate superior performance over various state-of-the-art methods.

2. Literature survey

P.A. Absil, R. Mahony, and R. Sepulchre [1] in Riemannian geometry of Grassmann manifolds with a view on algorithmic computation given simple formulas for the canonical metric, gradient, Riemannian connection, Lie derivative, parallel translation, geodesics and distance on the Grassmann manifold of p-planes in \mathbb{R}^n . In these formulas, p-planes are represented as the column space of $n \times p$ matrices. The Newton method on Riemannian manifolds proposed by S. T. Smith is made explicit on the Grassmann manifold. Two applications –computing an invariant subspace of a matrix and the mean of subspaces and considered the Grassmann manifold $\text{Grass}(p, n)$ of p-planes in \mathbb{R}^n as the base space of a GLp-principal fiber bundle with the noncompact Stiefel manifold $\text{ST}(p, n)$ as total space. Using the essentially unique On-invariant metric on $\text{Grass}(p, n)$, we have derived a formula for the Levi-Civita connection in terms of horizontal lifts. Moreover, formulas have been given for the Lie bracket, parallel translation, distance and geodesics between p-planes. Finally, these results have been applied to a detailed derivation of the Newton method on the Grassmann manifold.

Timo Ahonen, Esa Rahtu, Ville Ojansivu, Janne Heikkila[3] in Recognition of Blurred Faces Using Local Phase Quantization given recognition of blurred faces using the recently introduced Local Phase Quantization (LPQ) operator is proposed. LPQ is based on quantizing and the Fourier transform phase in local neighborhoods. The segment can be shown to be a blur invariant property under certain commonly fulfilled situations. In face image analysis, histograms of LPQ labels computed within local regions are used as a face descriptor similarly to the widely used Local Binary Pattern (LBP) methodology for face image description.

A. Chakrabarti, T. Zickler, and W. Freeman [6] in Analyzing spatially-varying blur, blur is caused by a pixel receiving light from multiple scene points, and in several cases, such as object motion, then make blur varies spatially across the image plane. Though, the seemingly straight-forward task of estimating spatially-varying blur from a single image has proved hard to accomplish reliably. This effort considers such blur and makes two contributions: a local blur cue that measures the likelihood of a small neighborhood being blurred by a candidate blur kernel; and an algorithm that, given an image, at the same time selects a motion blur kernel

and segments the region that it affects. The methods are performed well on a diversity of images.

3. Space of Blur and Blur-Invariants

The goal of this section is to obtain a representation of an image y that is invariant to blurring with arbitrary k , under three assumptions: (i) there is no noise in the system ($\eta = 0$), (ii) the maximum size of the blur kernel $b_1 \times b_2 = N$ is known, and (iii) the $N \times N$ BTTB matrix corresponding to the unknown blur PSF, under 0 boundary conditions for convolution, is full rank. More discussions on these assumptions are provided in the later part of this section.

For the case of 2D signals, we write any square integrable,

shift-invariant kernel k of size $b_1 \times b_2$ as, $k = \sum_{i=1}^N \alpha_i \phi_i$,

where $\{\phi_i\}_{i=1}^N$ is a complete set of orthonormal basis functions for $\mathbb{R}^{b_1 \times b_2}$, and $\{\alpha_i\}_{i=1}^N$ are their combining coefficients. Hence under no noise, (1) becomes,

$$\tilde{y} = y * \sum_{i=1}^N \alpha_i \phi_i \tag{2}$$

where the specific form of k is determined by $\{\alpha_i\}_{i=1}^N$. We now create a dictionary

$$D(y) = [(y * \phi_1)^v (y * \phi_2)^v \dots (y * \phi_N)^v] \tag{3}$$

Of size $d \times N$, where $d = d_1 \times d_2$ with $d > N$, and $(\cdot)^v$ denotes the vectorization operation. The column span of $D(y)$ is a subspace containing the set of convolutions of y with arbitrary kernels of maximum size $b_1 \times b_2$. (i.e.) $\text{span}(D(y)) = \mathcal{Y} = \{y * k | k \in \mathbb{R}^{b_1 \times b_2}\}$, which is an N -dimensional subspace in \mathbb{R}^d . It is important to note here that the set of all blurred images of y (produced by convolving y with physically realizable blur kernels that have non-negative co-efficients summing to one), span only a part of this subspace.

Proposition 3.1: $\text{span}(D(y))$ is a blur-invariant of y . In other words, $\text{span}(D(y)) = \text{span}(D(\tilde{y}))$, where \tilde{y} is a blurred version of y .

Proof: Let $\Phi = [(\phi_1)^v (\phi_2)^v \dots (\phi_N)^v]$ denote the $N \times N$ orthonormal matrix created from the basis functions. By writing convolution as matrix multiplication, (3) becomes $D(y) = Y\Phi$, where Y is a $d \times N$ matrix. The rows of Y are created by arranging the elements of y such that their multiplication with a ϕ_i will realize the effect of convolution (of y with ϕ_i) at all d corresponding pixels. Since Φ is full rank, $\text{span}(D(y)) = \text{span}(Y)$.

Now to prove Proposition 3.1, let us consider k_s to be the unknown blur kernel of (maximum) size $b_1 \times b_2$ that produced \tilde{y} from a clean image y . From (3) we have,

$$D(\tilde{y}) = [(\tilde{y} * \phi_1)^v \dots (\tilde{y} * \phi_N)^v] = [(y * k_S * \phi_1)^v \dots (y * k_S * \phi_N)^v]$$

$$= Y[(k_S * \phi_1)^v (k_S * \phi_2)^v \dots (k_S * \phi_N)^v] = YK_S\Phi \quad (4)$$

where K_S is the BTTB matrix of size $N \times N$ corresponding to the kernel k_S . Since the column span of $D(\tilde{y})$ and $D(y)$ is same if K_S is full rank, $\text{span}(D(y)) = Y$ is a blur-invariant.

Discussion: (i) One main advantage offered by this approach is that, since the basis functions can span any blur function of a known maximum size, we do not have constraints on the shape of blur functions that can be handled (unlike other invariants). (ii) Regarding the assumption on the rank of K_S , we would like to stress that although some blur PSF's are not invertible, their BTTB matrices are generally full rank (see [16], and the references therein). These BTTB matrices, however, can be extremely ill-conditioned at times. But since we do not invert these matrices, we do not encounter problems related to high condition numbers of matrix inversion that are prevalent in deblurring-based approaches. (iii) We note that there always exist practical scenarios such as the nonzero measurement noise that render some of our assumptions invalid. We present an analysis on the robustness of the invariant to additive perturbations in the supplementary material.

4. Face Recognition Across Blur

We now study the utility of invariant Y for the problem of recognizing faces across blur, where we empirically evaluate its robustness to sensor-related noise and the presence of other intra-class facial variations between the gallery and probe. Let us consider an M class problem with $\{y_i\}_{i=1}^M$ denoting the gallery faces, either clean or blurred, belonging to all subjects. Let \tilde{y} denote the blurred probe image which belongs to one of the M classes. The problem we are looking at is, given y_i 's and \tilde{y} , find the identity $i^* \in \{1, 2, \dots, M\}$ of \tilde{y} . From the gallery and probe, we first create their respective dictionaries $D(y_i)$'s and $D(\tilde{y})$ using (3), and then compare their column span, \mathcal{Y}_i 's and $\tilde{\mathcal{Y}}$ respectively, to perform recognition.

4.1 Grassmann Manifold: Definition and some methodologies for recognition

Since we are comparing linear subspaces in \mathbb{R}^d of dimension N , the problem of recognition can be recast as a recognition problem over the Grassmann manifold. The Grassmannian $\mathbb{G}_{N,d}$ is an analytical manifold that corresponds to the space of all N - dimensional subspaces in \mathbb{R}^d containing the origin. The blur-invariant Y is a point on $\mathbb{G}_{N,d}$. An illustration is provided in Figure 1. Understanding the geometric properties of the Grassmann manifold has been the focus of works like [33], [8], [1], and these have been utilized in some vision problems with subspace constraints, e.g. [5], [15], [21]. A compilation of statistical analysis methods on this manifold can be found in [7]. Since a full-fledged explanation of these methods is beyond the scope of this short paper, we refer the interested readers to the papers mentioned above. We now

use some of these results to compute the distance between the blur-invariants. We specifically focus on the following two cases.

4.1.1 Finding distance between points on $\mathbb{G}_{N,d}$

The first method uses the distance between points on the manifold for classification, which has more relevance when the gallery contains only one image per person. Formally, the Riemannian distance between two subspaces, say \mathcal{Y}_1 and \mathcal{Y}_2 , is the length of the shortest geodesic connecting those points on the Grassmann manifold. One way of obtaining this length is to compute the direction (velocity) matrix A such that the geodesic along that direction, while starting at \mathcal{Y}_1 , reaches \mathcal{Y}_2 in unit time. A is computed using the inverse exponential map. However, since the expression for the inverse exponential map is not available analytically for the Grassmann manifold, we use a numerical method [14] as given in Algorithm 1. The length of A gives the distance d_G between \mathcal{Y}_1 and \mathcal{Y}_2 , and we use $\text{trace}(AA^T)$, where $(\cdot)^T$ is the transpose operator, as the metric to compute the length. More formally, if $A^{\mathcal{Y}_1, \mathcal{Y}_2}$ is the direction matrix between \mathcal{Y}_1 and \mathcal{Y}_2 .

$$d_G(\mathcal{Y}_1, \mathcal{Y}_2) = \text{trace}(A^{\mathcal{Y}_1, \mathcal{Y}_2} A^{\mathcal{Y}_1, \mathcal{Y}_2 T}) \quad (5)$$

We then perform recognition with d_G using a nearest neighbor classifier.

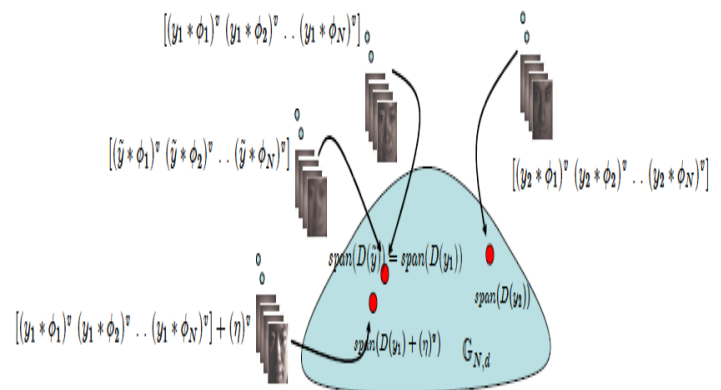


Fig. 1. Representing the blur-invariants as points on the Grassmann manifold $\mathbb{G}_{N,d}$. Given two subjects, y_1 and y_2 , and the blurred test face \tilde{y} belonging to subject 1, we illustrate how the \mathcal{Y}_i 's, created from them lie on the Grassmann. $\mathcal{Y}_1 = \text{span}(D(y_1))$ and $\tilde{\mathcal{Y}} = \text{span}(D(\tilde{y}))$ map to the same point, while $\text{span}(D(y_1) + \eta)$, where the noise is due to different lighting, lies closer to $\text{span}(D(y_1))$ than $\text{span}(D(y_2))$. (All figures are best viewed in color).

Given two dictionaries $D(y_1)$ and $D(y_2)$ whose column space is a point on $\mathbb{G}_{N,d}$, we determine the velocity matrix A such that travelling in this direction from \mathcal{Y}_1 leads to \mathcal{Y}_2 in unit-time. Let $\bar{D}(y_1)$ and $\bar{D}(y_2)$ denote the $d \times N$ matrices obtained by orthonormalizing the columns of $D(y_1)$ and $D(y_2)$ respectively.

- Compute the $d \times d$ orthogonal completion Q of $D(y_1)$.
- Compute the thin CS decomposition of $Q^T \bar{D}(y_2)$,

$$Q^T \bar{D}(y_2) = \begin{pmatrix} X_C \\ Y_C \end{pmatrix} = \begin{pmatrix} U_1 & 0 \\ 0 & \bar{U}_2 \end{pmatrix} \begin{pmatrix} \Gamma(1) \\ -\Sigma(1) \end{pmatrix} V_1^T$$
- Compute $\{\bar{\phi}_i\}$ which are given by the arcsine and arccos of the diagonal elements of Γ and Σ respectively, i.e. $\gamma_i = \cos(\bar{\phi}_i)$, $\sigma_i = \sin(\bar{\phi}_i)$. Form the diagonal matrix $\bar{\Phi}$ containing $\bar{\phi}_i$'s as diagonal elements.
- Compute $A = \bar{U}_2 \bar{\Phi} U_1$.

Algorithm 1: Numerical computation of the velocity matrix: The inverse exponential map [14].

From the gallery faces y_i 's constituting M classes, and probe faces \tilde{y}_i , compute the respective dictionaries $D(y_i)$ and $D(\tilde{y}_i)$. Orthonormalize their columns to obtain $\bar{D}(y_i)$ and $\bar{D}(\tilde{y}_i)$.

Training:

- Compute the matrix $[K_{train}]_{ij} = k_P(D(y_i), D(y_j))$ for all $\bar{D}(y_i), \bar{D}(y_j)$ in the training set, where k_P is the projection kernel defined earlier.
- Solve $\max_{\gamma} L(\gamma)$ by eigen-decomposition (6), with $K^* = K_{train}$.
- Compute the $(M-1)$ -dimensional coefficients, $F_{train} = \gamma^T K_{train}$

Testing:

- Compute the matrix $[K_{test}]_{ij} = k_P(\bar{D}(y_i), \bar{D}(\tilde{y}_j))$ for all $D(y_i)$ in training, and $D(\tilde{y}_j)$ in testing.
- Compute $(M-1)$ -dimensional coefficients, $F_{test} = \gamma^T K_{test}$ by solving for (6) with $K^* = K_{test}$.
- Perform 1-NN classification from the Euclidean distance between F_{train} and F_{test}

The Rayleigh quotient $L(\gamma)$ is given by,

$$L(\gamma) = \max_{\gamma} \frac{\gamma^T K^* (V - 1_B 1_B^T / B) K^* \gamma}{\gamma^T (K^* (I_B - \bar{V}) K^* + \sigma^2 I_B) \gamma} \quad (6)$$

where K^* is the Gram matrix (K_{train} or K_{test}), 1_B is a uniform vector $[1 \dots 1]^T$ of length B corresponding to the number of gallery images, \bar{V} is the block-diagonal matrix whose m^{th} block ($m = 1$ to M) is the uniform matrix $1_{B_m} 1_{B_m}^T / B_m$, B_m is the number of gallery images in m^{th} class, and $\sigma^2 I_B$ is a regularizer to make computations stable.

Algorithm 2: Kernel Linear Discriminant Analysis (KLDA) [15].

4.1.2 Learning from data on $\mathbb{G}_{N,d}$

In cases where there is more data available for each person in the gallery portraying other intra-class facial variations, it paves the way for performing statistics on the point cloud on $\mathbb{G}_{N,d}$. Since the blur-invariants have a resultant dimension of $(d - N) \times N$ [8], with d significantly higher than N , it would require large number of samples to learn class-specific distributions. We hence pursued the method of Hamm and

Lee [15] that performs kernel linear discriminant analysis on the blur-invariants using the projection kernel $k_P(\bar{D}(y_1), \bar{D}(y_2)) = \|\bar{D}(y_1)^T \bar{D}(y_2)\|_F^2 = \text{trace}[(\bar{D}(y_1) \bar{D}(y_1)^T)(\bar{D}(y_2) \bar{D}(y_2)^T)]$, which is a Mercer kernel that implicitly computes the inner product between $\bar{D}(y_i)$'s in the space obtained using the following embedding; $\omega_P : \mathbb{G}_{N,d} \rightarrow \mathbb{R}^{d \times d}$, $\text{span}(\bar{D}(y_i)) \rightarrow \bar{D}(y_i) \bar{D}(y_i)^T$. To make the paper self-contained, we present the details of this method in Algorithm 2.

4.2 Performing Recognition across Blur

4.2.1 Spatially uniform blur

In the case when k remains unchanged over all pixels (n_1, n_2) of a $d_1 \times d_2$ image y (1), recognition is performed by a nearest neighbor classifier on the two distances (say, SD) discussed before namely, (i) the Riemannian distance d_G (5), and (ii) the Euclidean distance in the lower-dimensional space obtained from KLDA (Algorithm 2). The identity of probe \tilde{y} is therefore obtained by,

$$i^* = \arg \min_i SD(D(\tilde{y}), D(y_i)) \quad (7)$$

4.2.2 Spatially varying blur

We now study the more difficult problem, where the blur kernel k is spatially varying. This occurs when different parts of the scene are affected differently by blur, with some common examples being; outof- focus blur in objects with depth discontinuities, and motion blur when there is a sudden change in intensity values of a region due to object movements. The image formation equation for this case can be written as,

$$\tilde{y}_n = y_n * k_n \quad (8)$$

where the subscript n indicates the pixel location. Since a blur kernel acts on a local spatial neighborhood, allowing it to change at every pixel location makes the problem severely under-constrained. A common assumption made to overcome this condition is to assume the blur to be locally uniform [6], which is valid in most practical cases. Along these lines, if the blur is assumed to be uniform over a region of size $d'_1 \times d'_2$ (with $d'_1 > b_1$, and $d'_2 > b_2$), we can perform recognition by dividing the image into T overlapping patches of $d'_1 \times d'_2$ each, and rewriting (7) as,

$$i^* = \arg \min_i \sum_{t=1}^T SD(D(\tilde{y})_t, D(y_i)_t) \quad (9)$$

where the subscript t denotes the patch at which the quantities in (9) are computed, and the span of $D(\cdot)_t$'s are points on $\mathbb{G}_{N,d'}$, $d' = d'_1 \times d'_2$. The inherent assumption while matching patches is that the faces are aligned. However for those patches where there is a transition between blur kernels, the column space of $D(\cdot)_t$ will not be invariant to

blur. The percentage of such instances depends on the nature of spatially varying blur.

5. Conclusion

We showed that the subspace resulting from convolutions of an image with a complete set of orthonormal basis functions that could represent the blur kernel is invariant to blur under some assumptions, and it can account for more general classes of blur unlike other invariants. We then studied the utility of this invariant for the problem of direct recognition of faces, using techniques that account for their underlying non-Euclidean geometry, and observed an improved performance over other existing deblurring-based and invariant-based approaches. From the point of view of performing robust face recognition under unconstrained settings, it is interesting to study the integration of explicit formulations of other facial variations such as lighting and pose, with this blur-invariant.

References

- [1] P.-A. Absil, R. Mahony, and R. Sepulchre. Riemannian geometry of Grassmann manifolds with a view on algorithmic computation. *Acta Appl. Math.*, 80:199–220, Feb. 2004.
- [2] A. Agrawal and Y. Xu. Coded exposure deblurring: Optimized codes for PSF estimation and invertibility. In *CVPR*, pages 2066–2073, June 2009.
- [3] T. Ahonen, E. Rahtu, V. Ojansivu, and J. Heikkilä. Recognition of blurred faces using local phase quantization. In *ICPR*, pages 1–4, Dec. 2008.
- [4] H. Andrews and B. Hunt. *Digital Image Restoration*. Prentice Hall Signal Processing Series, 1977.
- [5] E. Begelfor and M. Werman. Affine invariance revisited. In *CVPR*, pages 2087–2094, June 2006.
- [6] A. Chakrabarti, T. Zickler, and W. Freeman. Analyzing spatially-varying blur. In *CVPR*, pages 2512–1519, June 2010.
- [7] Y. Chikuse. *Statistics on special manifolds*. Springer Verlag, 2003.
- [8] A. Edelman, T. Arias, and S. Smith. The geometry of algorithms with orthogonality constraints. *SIAM Journal of Matrix Analysis and Application*, 20:303–353, Apr. 1999.
- [9] R. Fergus, B. Singh, A. Hertzmann, S. T. Roweis, and W. T. Freeman. Removing camera shake from a single photograph. *ACM Transactions on Graphics*, 25:787–794, Mar. 2006.
- [10] J. Flusser, J. Boldys, and B. Zitova. Moment forms invariant to rotation and blur in arbitrary number of dimensions. *IEEE TPAMI*, 25:234–246, Feb. 2003.
- [11] J. Flusser, J. Boldy’s, and B. Zitova. Invariants to convolution in arbitrary dimensions. *Journal of Mathematical Imaging and Vision*, 13:101–113, Feb. 2000.
- [12] J. Flusser and T. Suk. Degraded image analysis: an invariant approach. *IEEE TPAMI*, 20:590–603, June 1998.
- [13] J. Flusser, T. Suk, and S. Saic. Recognition of images degraded by linear motion blur without restoration. In *Proc. Theoretical Foundations of Computer Vision*, pages 37–51, Sep. 1996.
- [14] K. Gallivan, A. Srivastava, X. Liu, and P. Van Dooren. Efficient algorithms for inferences on grassmann manifolds. In *Workshop on Statistical Signal Processing*, pages 315–318, Feb 2003.
- [15] J. Hamm and D. D. Lee. Grassmann discriminant analysis: a unifying view on subspace-based learning. In *ICML*, pages 376–383, July 2008.
- [16] P. C. Hansen, J. G. Nagy, and D. P. O’Leary. *Deblurring Images: Matrices, Spectra, and Filtering*. Society for Industrial and Applied Mathematics, Philadelphia, PA, USA, 2006.
- [17] H. Hu and G. de Haan. Low cost robust blur estimator. In *ICIP*, pages 617–620, Oct. 2006.
- [18] K. Lee, J. Ho, and D. Kriegman. Acquiring linear subspaces for face recognition under variable lighting. *IEEE TPAMI*, 27:684–698, May 2005.
- [19] A. Levin, D. Lischinski, and Y. Weiss. A closed-form solution to natural image matting. *IEEE TPAMI*, 30:228–242, Feb. 2008.
- [20] A. Levin, Y. Weiss, F. Durand, and W. Freeman. Efficient marginal likelihood optimization in blind deconvolution. In *CVPR*, pages 2657–2664, June 2011.
- [21] Y. M. Lui and J. R. Beveridge. Grassmann registration manifolds for face recognition. In *ECCV*, pages 44–57, Oct. 2008.
- [22] M. Nishiyama, A. Hadid, H. Takeshima, J. Shotton, T. Kozakaya, and O. Yamaguchi. Facial deblur inference using subspace analysis for recognition of blurred faces. *IEEE TPAMI*, 33:838–845, Apr. 2011.
- [23] M. Nishiyama, H. Takeshima, J. Shotton, T. Kozakaya, and O. Yamaguchi. Facial deblur inference to improve recognition of blurred faces. In *CVPR*, pages 1115–1122, June 2009.
- [24] V. Ojansivu and J. Heikkila. A method for blur and affine invariant object recognition using phase-only bispectrum. In *ICIAR*, pages 527–536, June 2008.
- [25] P. Phillips, P. Flynn, T. Scruggs, K. Bowyer, J. Chang, K. Hoffman, J. Marques, J. Min, and W. Worek. Overview of the face recognition grand challenge. In *CVPR*, pages 947–954, June 2005.
- [26] P. Phillips, H. Moon, S. Rizvi, and P. Rauss. The FERET evaluation methodology for face-recognition algorithms. *IEEE TPAMI*, 22:1090–1104, Oct. 2000.
- [27] L. I. Rudin, S. Osher, and E. Fatemi. Nonlinear total variation based noise removal algorithms. *Physica D*, 60:259–268, Nov. 1992.
- [28] T. Sim, S. Baker, and M. Bsat. The CMU pose, illumination, and expression database. *IEEE TPAMI*, 25:1615–1618, Dec. 2003.
- [29] I. Stainvas and N. Intrator. Blurred face recognition via hybrid network architecture. In *ICPR*, pages 805–808, Sep 2000.
- [30] T. Suk and J. Flusser. Combined blur and affine moment invariants and their use in pattern recognition. *Pattern Recognition*, 36:2895–2907, Dec. 2003.
- [31] A. N. Tikhonov and V. Y. Arsenin. *Solutions of Ill-Posed Problems*. V. H. Winston & Sons, Washington, D.C.: John Wiley & Sons, New York., 1977.
- [32] P. Turaga, A. Veeraraghavan, A. Srivastava, and R. Chellappa. Statistical computations on grassmann and

stiefel manifolds for image and video-based recognition.

IEEE TPAMI, 33:2273–2286, Nov. 2011.

- [33] Y. Wong. Differential Geometry of Grassmann Manifolds. Proc. of the National Academy of Science, 57:589–594, 1967.
- [34] L. Yuan, J. Sun, L. Quan, and H.-Y. Shum. Progressive interscale and intra-scale non-blind image deconvolution. ACM Transactions on Graphics, 27:1–10, Mar. 2008.

Author Profile



Mr. Ankush Jain [M.Tech] working as assistant professor in Computer Science Engineering from CVSR COLLEGE OF ENGINEERING from ANURAG GROUP OF INSTITUTIONS Venkatapur(V), Ghatkesar(M), Ranga Reddy District,

Hyderabad-500088, Telangana State.



P. Santhosh Kumar received the B.Tech degree in Computer Science and Engineering from JNTU Hyderabad 2011 and pursuing M.Tech Degree in Computer science and Engineering from JNTU

Hyderabad.